

05,07

Effect of oxygen content variations on structural and magnetic features in $\text{La}_{0.5}\text{Sr}_{0.5}\text{FeO}_{3-\delta}$

© A.I. Dmitriev¹, S.V. Zaitsev², M.S. Dmitrieva¹, O.G. Rybchenko², V.D. Sedykh²¹ Federal Research Center of Problems of Chemical Physics and Medicinal Chemistry RAS, Chernogolovka, Russia² Osipyan Institute of Solid State Physics RAS, Chernogolovka, Russia

E-mail: aid@icp.ac.ru

Received January 11, 2024

Revised January 28, 2024

Accepted February 4, 2024

The dependences of the magnetic moment on the temperature $M(T)$ and the magnetic field strength $M(H)$ of polycrystalline samples $\text{La}_{0.5}\text{Sr}_{0.5}\text{FeO}_{3-\delta}$ before and after vacuum annealing are studied in detail. Four critical temperatures are visible on the curves $M(T)$ of the sample before annealing. The temperature $T_1 = T_N \approx 230$ K corresponds to the Néel temperature of the compound $\text{La}_{0.5}\text{Sr}_{0.5}\text{FeO}_{3-\delta}$, at which a weak „parasitic“ ferromagnetism is established in the sample. The temperature $T_2 = T_V \approx 195$ K corresponds to the Verwey temperature, below which the localization of charge carriers occurs in the sample. The temperature range from $T_3 \approx 170$ K to $T_4 \approx 80$ K apparently corresponds to the formation of a frustrated spin glass state in the sample. Vacuum annealing leads to a noticeable increase in the Néel temperature T_N . The magnetometry data are also confirmed by the data of Mössbauer and Raman spectroscopy.

Keywords: orthoferrites, canted antiferromagnetism, vacuum annealing.

DOI: 10.61011/PSS.2024.03.57939.1

1. Introduction

For the last two decades the perovskites $\text{La}_{1-x}\text{Sr}_x\text{FeO}_{3-\delta}$ ($0 \leq x \leq 1$) have attracted significant attention due to a wide range of interesting physical properties [1–4]. They can be used, for example, as an oxygen-storage material [5] and as a membrane material in methane partial oxidation reactors, to provide for high values of CO selectivity and conversion CH_4 [6,7].

The compounds of the composition ABO_3 (A — rare earth elements B — metals) have a perovskite-like crystal structure. When Fe ions are used as the metal (B) in them, these compounds are called orthoferrites AFeO_3 . This family of orthoferrites includes lanthanum ferrite LaFeO_3 , which has a rhombic structure. The Fe ions therein are in a trivalent state Fe^{3+} . The compound is an antiferromagnetic insulator with the Néel temperature $T_N = 740$ K [8]. The antiferromagnetics also include strontium ferrite SrFeO_3 with $T_N = 134$ K [8,9], which has a cubic symmetry. The Fe ions therein are in a four-valence state Fe^{4+} . In both compounds, the magnetic properties are attributable to superexchange interaction due to overlapping of wave functions of the $3d$ -orbitals of magnetic ions and the p -orbitals of oxygen ions. In accordance with the Goodenough theory, the superexchange interaction between the ions Fe^{3+} is antiferromagnetic, while that between the ions Fe^{4+} and Fe^{3+} , and the ions Fe^{4+} as well is ferromagnetic [8]. It is important to note that the antiferromagnetic superexchange is stronger than the ferromagnetic one [8].

It was found that substitution of La^{3+} by Sr^{2+} in LaFeO_3 increased its electron conductivity and decreased T_N [8]. Another result of ionic substitution of La^{3+} by Sr^{2+} is appearance of the ions Fe^{4+} , i.e. a mixed valence state of the ions Fe^{3+} and Fe^{4+} is formed. That is why the substituted orthoferrites $\text{La}_{1-x}\text{Sr}_x\text{FeO}_{3-\delta}$ are called mixed valence oxides [10]. The substitution of La^{3+} by Sr^{2+} results in the weakened superexchange interaction between the ions Fe^{3+} , because the ions Fe^{4+} and the oxygen vacancies appear. One of the most interesting properties of the series of the substituted orthoferrites $\text{La}_{1-x}\text{Sr}_x\text{FeO}_{3-\delta}$ is manifested at the concentration $x = 2/3$. The samples $\text{La}_{1/3}\text{Sr}_{2/3}\text{FeO}_{3-\delta}$ undergo a metal-insulator transition, which is indicated by a jump of resistivity by more than an order with temperature reduction. It is interpreted as suppression of the electron transfer process with charge ordering at the temperatures below the Verwey transition $T_V = 210$ K [11,12]. In accordance with some literature data, the Fe ions are transformed from the state of average valence $\text{Fe}^{(+3.67)}$ at the paramagnetic phase above 210 K into the mixture 2Fe^{3+} and 1Fe^{5+} at the antiferromagnetic state with charge ordering below 210 K. In turn, Fe^{5+} is formed as a result of disproportionation of Fe^{4+} into Fe^{3+} and Fe^{5+} [2,3,13]. However, according to the Mössbauer data, there is no data confirming the presence of Fe^{5+} [14,15].

The present paper has been aimed at: establishing types of the magnetic ordering in $\text{La}_{0.5}\text{Sr}_{0.5}\text{FeO}_{3-\delta}$ and determining temperature ranges of existence thereof, separation of

contributions of various magnetic phases to magnetization of $\text{La}_{0.5}\text{Sr}_{0.5}\text{FeO}_{3-\delta}$, and tuning of the magnetic properties of $\text{La}_{0.5}\text{Sr}_{0.5}\text{FeO}_{3-\delta}$ by heat treatment.

2. Methods and material

The sample $\text{La}_{0.5}\text{Sr}_{0.5}\text{FeO}_{3-\delta}$ has been synthesized by a sol-gel method using Sr, Fe and La nitrates in a stoichiometric ratio as initial reagents. After the synthesis, a portion of the powder sample was annealed in vacuum (10^{-3} Torr) at 650°C for 6 h to reduce oxygen concentration in the crystal lattice. The preparation is detailed in the papers [16,17].

The paper [17] describes in detail results of X-ray diffraction analysis. There are extensively widened lines of the X-ray patterns of the unannealed sample unlike the sample annealed at 650°C . It can be related both to a very small size of crystallites and heterogeneous distribution of oxygen over the sample. It has been established that the initially produced orthoferrite $\text{La}_{0.5}\text{Sr}_{0.5}\text{FeO}_{3-\delta}$ has a rhombohedral structure with the lattice parameters $a = 5.511 \text{ \AA}$, $c = 13.437 \text{ \AA}$ in the hexagonal axes ($a = 5.494 \text{ \AA}$ and $\alpha = 60.20^\circ$ in the rhombohedral axes). Vacuum annealing of the initial orthoferrite at the temperature 650°C results in the transition of the structure to the cubic one with $a = 3.914 \text{ \AA}$. According to the Mössbauer data, the process undergoing under vacuum annealing can be characterized as a change of local environment of the ions Fe^{3+} towards reduction of its distortion.

The dependencies of magnetic moment on the temperature $M(T)$ and the magnetic field strength $M(H)$ have been measured using a vibration magnetometer of the multifunctional measurement cryomagnetic device CFMS manufactured by Cryogenic Ltd, UK.

The spectra of the Mössbauer absorption of ^{57}Fe were measured at the temperatures 85 and 300 K in a transmission geometry using the spectrometer SM 1101 (Russia) operating in a mode of constant acceleration. ^{57}Co in a Rh matrix was used as a source of γ -quanta. The values of isomer shift are taken in relation to $\alpha\text{-Fe}$ — which is a standard Mössbauer absorber. The source of the γ -quanta and the standard absorber were at room temperature. All the Mössbauer spectra were processed within the framework of the software package SpectrRelax [18].

The Raman scattering spectra were measured at room temperature in a backscattering geometry. It was excited using a laser of the wavelength 532 nm with the laser radiation power $\sim 3 \text{ mW}$. A diameter of the laser spot focused by a microscope lens ($\times 50$) on the sample was $\sim 2\text{--}3 \mu\text{m}$. The laser line was suppressed by using a step filter of anti-Stokes' cut-off placed in front of the spectrometer. The spectral resolution within the studied frequency range is at least 1 cm^{-1} at the absolute measurement accuracy $\pm 1 \text{ cm}^{-1}$.

3. Results and discussion

3.1. Unannealed initial sample

Figure 1 shows the temperature dependencies of magnetization $M(T)$ of the sample, which were measured in various magnetic fields, and the dependencies $M(T)$, which were measured in the ZFC and FC modes before vacuum annealing. The curves $M(T)$ clearly shows four critical temperatures. The temperature $T_1 \approx 230 \text{ K}$ corresponds to flexion of the curves $M(T)$, which is well visualized using the derivative dM/dT . The curves FC-ZFC start diverging below T_1 . The temperature $T_2 \approx 195 \text{ K}$, at which there is a maximum observed at the curves $M(T)$, measured in the ZFC mode in the magnetic field of the strength 1 kOe, and under cooling in the magnetic fields of the strength 5 and 10 kOe.

The temperature range $T_3 \approx 160\text{--}180 \text{ K}$ corresponds to the temperatures of the minimums at the curves $M(T)$, measured in the ZFC mode in the magnetic field of the strength 1 kOe, and under cooling in the magnetic field of the strength 5 and 10 kOe. At the same time, the higher the strength of the magnetic field, the lower T_3 . The temperature $T_4 \approx 80 \text{ K}$ corresponds to the second low-temperature maximum on the curve $M(T)$, measured in the ZFC mode.

The curves, which are similar to those shown in Figure 1, had been previously observed in the substituted orthoferrites $\text{La}_{1-x}\text{Sr}_x\text{FeO}_{3-\delta}$ with the antiferromagnetic structure [1,3,14,19]. Spins therein are arranged antiparallel due to an antiferromagnetic bond between two neighboring Fe ions via an intermediate ion of oxygen. However, due to slight deviation of the spins from rigorous antiparallel orientation, which results from zig-zag arrangement of Fe ion-containing octahedrons along the axis c , the samples exhibit weak („parasitic“) ferromagnetism [20]. Indeed, the curves $M(T)$ exhibit a significant ferromagnetic component

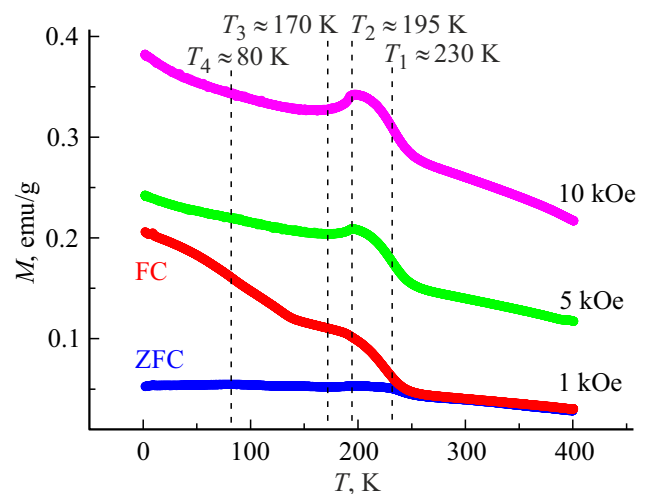


Figure 1. Temperature dependencies of magnetization $M(T)$ of the sample before annealing.

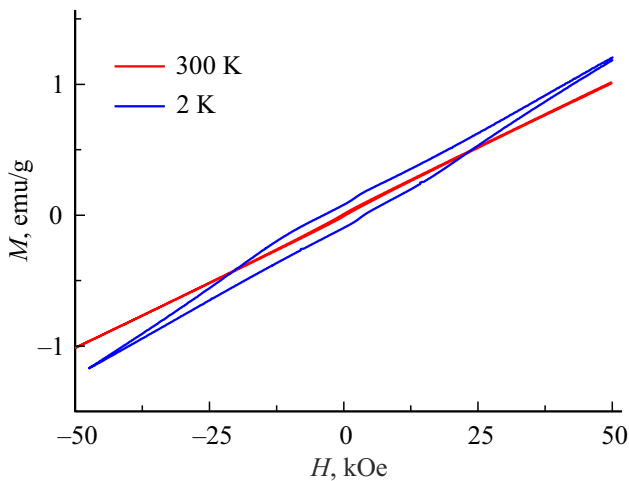


Figure 2. Magnetic hysteresis loops at the temperatures $T = 2$ K and 300 K of the sample before annealing.

(Figure 1), whose presence is also confirmed by hysteresis on the curves $M(H)$ (Figure 2). So, the temperature $T_N = T_1 \approx 230$ K corresponds to the Néel temperature of the substituted orthoferrite $\text{La}_{0.5}\text{Sr}_{0.5}\text{FeO}_{3-\delta}$.

At room temperature, the unannealed initial sample is a paramagnetic, which is indicated by a linear form of the dependencies $M(H)$ (Figure 2). The dependence $M(H)$ in the paramagnetics is described by the Brillouin function, which is degenerated into a straight line at the high temperatures.

The paramagnetic state of the synthesized sample at room temperature is confirmed by the data of Mössbauer spectroscopy. The detailed Mössbauer studies of the composition $\text{La}_{0.5}\text{Sr}_{0.5}\text{FeO}_{3-\delta}$ are given in the paper [17]. The present paper uses a necessary fragment of the results.

The paramagnetic state at room temperature is associated with a quadrupole doublet with hyperfine parameters: the isomer shift $IS \approx 0.18$ mm/s, the quadrupole shift of the doublet $\Delta \approx 0.09$ mm/s (Figure 3). The value of isomer shift indicates that at room temperature the Fe ions are in an average-valence state, i.e. they have a fractional part of oxidation between $3+$ and $4+$. This average-valence state of the ions Fe is due to fast (with the characteristic time $< 10^{-8}$ s) electron transfer between the ions Fe^{3+} and Fe^{4+} at room temperature, so the ions Fe^{4+} in the substituted ferrites do not exhibit in the Mössbauer spectra measured at room temperature [21].

A pronounced peak of the curve $M(T)$ had been previously observed in the paper [1], wherein showing that the same temperature has a jump on the temperature dependence of the electric resistivity. So, the temperature $T_V = T_2 \approx 195$ K corresponds to the Verwey temperature, below which the electron transfer process is suppressed in the sample $\text{La}_{0.5}\text{Sr}_{0.5}\text{FeO}_{3-\delta}$.

The fact that $T_V = T_2 \approx 195$ K corresponds to localization of the charge carriers is confirmed by the data of the Mössbauer spectroscopy. The Mössbauer spectrum of

the synthesized $\text{La}_{0.5}\text{Sr}_{0.5}\text{FeO}_{3-\delta}$, measured at 85 K, is a collection of several partial spectra in the form of Zeeman sextets, one of which with the smaller isomer shift ($IS \approx -0.06$ mm/s) and the hyperfine magnetic field ($H_{\text{hf}} \approx 260$ kOe) can be related to the ions Fe^{4+} , and the rest to the ions Fe^{3+} ($H_{\text{max}} \approx 553$ kOe, $IS \approx 0.43$ mm/s) (Figure 4).

So, there is no average-valence state of the Fe ions observed at the low temperatures. It indicates freezing of the electron transfer process. No partial spectrum for the Fe^{5+} ions in the substituted lanthanum ferrite's spectrum does not allow accepting interpretation with the disproportionation and the charge ordering [2,3,13].

The samples $\text{La}_{1/3}\text{Sr}_{2/3}\text{FeO}_{3-\delta}$ undergo a similar transition at $T_V = 210$ K [11,12]. I.e. the temperature T_V is sensitive to the content of Sr. It is known that when the large cations Sr^{2+} are introduced, the length of the bond Fe–O is decreased. This feature enhances the antiferromagnetic superexchange interaction (J_{AF}). On the other hand, formation of the ions Fe^{4+} as a result of substitution of La^{3+} by Sr^{2+} results in the ferromagnetic exchange interaction (J_{F}) between the ions Fe^{3+} and the ions Fe^{4+} [12]. Besides, as was noted above, the slight slopes of the octahedrons

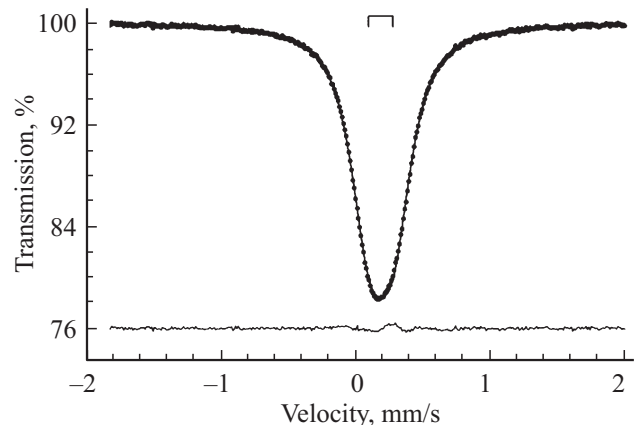


Figure 3. 300-K Mössbauer spectrum of the synthesized sample $\text{La}_{0.5}\text{Sr}_{0.5}\text{FeO}_{3-\delta}$.

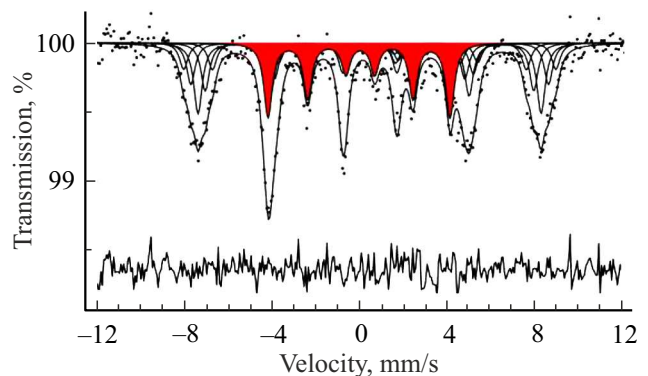


Figure 4. 85-K Mössbauer spectrum of the synthesized sample $\text{La}_{0.5}\text{Sr}_{0.5}\text{FeO}_{3-\delta}$.

also contribute to the ferromagnetic interaction. Since the state of charge ordering is stabilized with participation of the magnetic interactions [2], the change of the ratio J_F/J_{AF} results in the change of T_V .

Presently, there is no unambiguous interpretation of origin of a maximum at T_3 on the curve $M(T)$, which follows T_V at temperature reduction. It is hypothesized that at $T_N = T_1 \approx 230$ K there are local antiferromagnetic fluctuations, while at T_3 there is a long-range magnetic order after localization of the charge carriers [22]. The dependence of the magnitude T_3 on the strength of the magnetic field, wherein the curve $M(T)$ was measured, and the low-temperature maximum on the curve $M(T)$ measured in the ZFC mode make it possible to suggest a frustrated spin glass state realized at the temperatures below $T_4 \approx 80$ K [23,24].

3.2. Sample annealed in vacuum at 650°C

Figure 5 shows the temperature dependencies of magnetization $M(T)$, which are measured in the ZFC and FC modes, for the sample annealed in vacuum at 650°C.

The curves $M(T)$ register the following changes under annealing. The temperature T_1 , which corresponds to the point of inflection and divergence of the FC-ZFC curves, noticeably exceeds room temperature. It means that the annealing results in the noticeable increase in the Néel temperature T_N of substituted orthoferrite $\text{La}_{0.5}\text{Sr}_{0.5}\text{FeO}_{3-\delta}$, which is still in a magnetic-ordered state at room temperature. This fact is confirmed by the magnetic hysteresis loop at room temperature (Figure 6). The curves $M(T)$ of the sample after annealing evidently stop exhibiting the features at the temperatures T_2 and T_3 (Figure 6). The low-temperature maximum on the curve $M(T)$, measured in the ZFC mode, which probably responds to the frustrated spin glass state, is shifted to $T_4 \approx 60$ K.

For the sample after annealing, the magnetic hysteresis loops have a characteristic bend in small fields, which corresponds to fast magnetic saturation of the ferromagnetic component, and smaller magnetization at the same value of H (Figure 6). The different behavior of the curves $M(H)$ can be explained as follows. Under vacuum annealing, the crystal lattice undergoes two mutually-dependent processes: the oxygen ion is removed with a vacancy formation, and the vacancy state of the Fe ions changes from $4+$ to $3+$.

The ion Fe^{4+} available in the nearest cation environment of the ion Fe^{3+} weakens the superexchange interaction, while at the same time the oxygen vacancy appearing in the nearest anion environment of the ion Fe^{3+} results in breaking of the exchange bond. Thus, vacuum annealing results in redistribution of the contributions of the ferromagnetic (J_F) and antiferromagnetic (J_{AF}) channels to the resulting exchange and shifts the equilibrium towards enhancement of antiferromagnetism. This, in turn, results in noticeable increase in the Néel temperature T_N , decrease in the magnetic hysteresis loop and appearance of the characteristic bend thereon, and to reduction of the magnetization value. Since

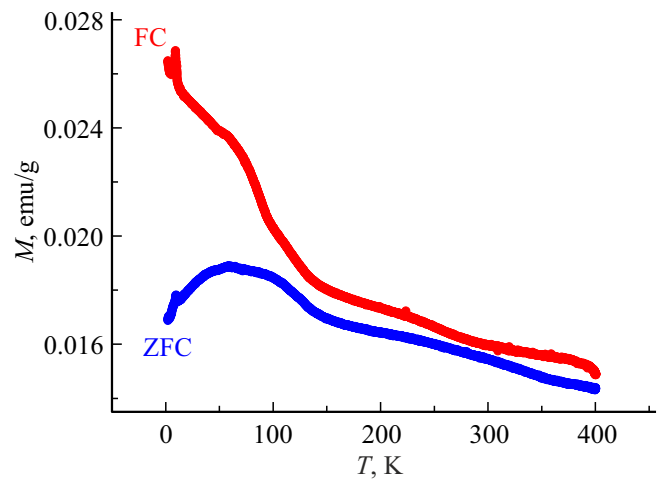


Figure 5. Temperature dependencies of magnetization $M(T)$ of the sample after annealing.

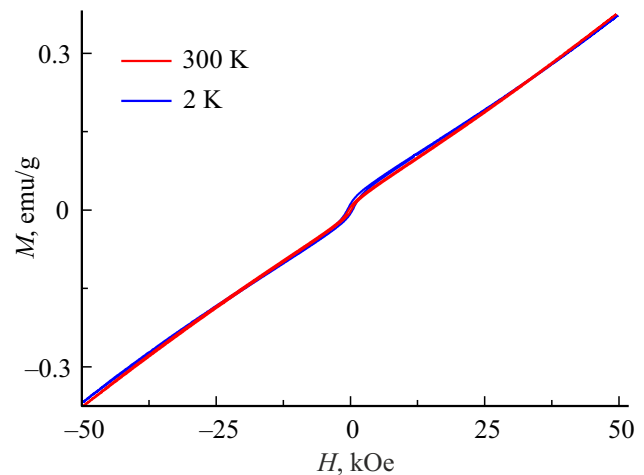


Figure 6. Magnetic hysteresis loops at the temperatures $T = 2$ K and 300 K of the sample after annealing.

the states of spin glass and charge ordering are stabilized with participation of the magnetic interactions, the change of the ratio J_F/J_{AF} results in suppression of the latter and reduction of spin glass freezing temperature T_f .

The magnetic-ordered state at room temperature of the sample $\text{La}_{0.5}\text{Sr}_{0.5}\text{FeO}_{3-\delta}$, annealed in vacuum at 650°C, is confirmed by the magnetic structures of the Mössbauer spectrum (Figure 7).

According to the results obtained, there is practically no Fe ion in the average-valence state in the sample. The spectrum lines are widened due to the local heterogeneity in the environment of the Mössbauer Fe atoms — the oxygen vacancies available in the structure. In accordance with the maximum value $IS_{\max} \approx 0.34$ mm/s, for the magnetic-ordered partial spectra, the Fe ions of the annealed sample are in the trivalent state of Fe^{3+} . The values $H_{\max} \approx 525$ kOe and IS_{\max} approach the values for the non-substituted lanthanum ferrite LaFeO_3 ($H_{\text{hf}} \approx 530$ kOe,

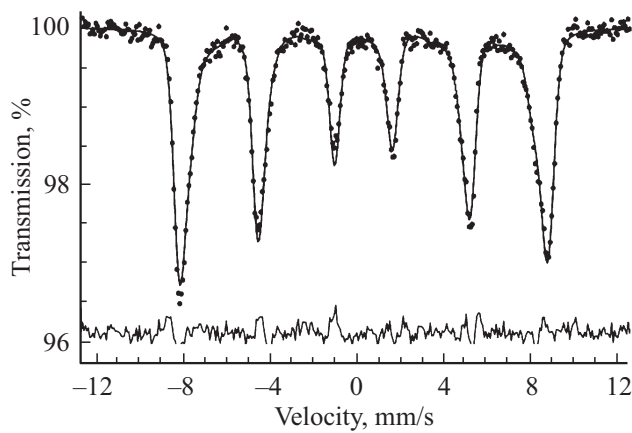


Figure 7. 300-K Mössbauer spectrum of the sample $\text{La}_{0.5}\text{Sr}_{0.5}\text{FeO}_{3-\delta}$ annealed in vacuum at 650°C .

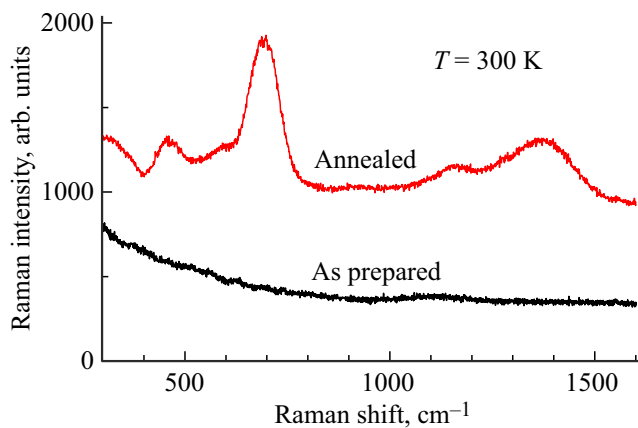


Figure 8. Light Raman scattering spectra at $T = 300^\circ\text{C}$ in the unannealed initial sample $\text{La}_{0.5}\text{Sr}_{0.5}\text{FeO}_{3-\delta}$ (black characters) and in the samples annealed in vacuum at 650°C (red characters).

$IS \approx 0.36 \text{ mm/s}$) [17]. Assuming the probabilities of the Mössbauer effect for the ^{57}Fe nuclei in the ions Fe^{3+} and Fe^{4+} to be almost the same, then at the fixed number of the ions $\text{Sr}^{2+}(x)$ relative areas of the partial spectra can be used to evaluate a number of the ions Fe^{4+} , the oxygen vacancies and the anions O_2 per formula unit. The estimations for the initial and annealed samples provide the compositions $\text{La}_{0.5}\text{Sr}_{0.5}\text{FeO}_{2.88}$ and $\text{La}_{0.5}\text{Sr}_{0.5}\text{FeO}_{2.76}$, respectively. The relative area of the Mössbauer partial spectrum associated with Fe^{4+} is the biggest for the unannealed initial sample [17]. Its area decreases with increase in the annealing temperatures and approaches zero at 650°C . The contributions of the partial spectra for the various states of Fe^{3+} are redistributed with increase in the annealing temperature. The relative area of the partial spectrum for the ions Fe^{3+} with all six exchange bonds $\text{Fe}^{3+}-\text{O}^{2-}-\text{Fe}^{3+}$ is significantly increased from the minimum value of 12% for the initial sample to $\sim 60\%$ for the sample annealed at 650°C in vacuum.

The antiferromagnetic type of ordering at room temperature in the sample $\text{La}_{0.5}\text{Sr}_{0.5}\text{FeO}_{3-\delta}$ annealed after the synthesis is indicated by a strong Raman peak of the two-magnon scattering at $\sim 1350-1400 \text{ cm}^{-1}$ available in the light Raman scattering spectra in Figure 8 [25]. The similar strong line of the two-magnon scattering is observed in the light Raman scattering spectra at room temperature in the antiferromagnetic lanthanum ferrite LaFeO_3 [26], which has the high Néel temperature $T_N = 740 \text{ K}$ [8].

Besides, at $\sim 1130 \text{ cm}^{-1}$ there is an intense line of two-phonon scattering, which exhibits due to strong relationship of the phonon and spin systems in these compounds [27]. At the frequencies below 1000 cm^{-1} the Raman lines in the light Raman scattering spectra of the orthoferrites $\text{La}_{1-x}\text{Sr}_x\text{FeO}_{3-\delta}$ are attributable to phonon oscillations [28]. So the strongest phonon mode at the frequency $\sim 690 \text{ cm}^{-1}$ describes in-phase oscillations of the bonds $\text{Fe}-\text{O}$ in the octahedron FeO_6 („breathing“ mode of the octahedron FeO_6) [28]. The substantial widening of all the lines of the light Raman scattering in $\text{La}_{0.5}\text{Sr}_{0.5}\text{FeO}_{3-\delta}$ in comparison to lanthanum ferrite LaFeO_3 [26] can be naturally associated with local disordering arising at substitution of La by Sr. An additional factor contributing to the disordering is the strong heterogeneity at the microscopic level for the charge state of the ions $\text{Fe}^{4+}/\text{Fe}^{3+}$ and the oxygen vacancies related thereto in the nearest environment of Fe, occurring under the vacuum annealing. Figure 8 also shows the light Raman scattering spectrum of the unannealed initial sample $\text{La}_{0.5}\text{Sr}_{0.5}\text{FeO}_{3-\delta}$, which has no magnon and phonon Raman peaks. Let us note that in this sample the full suppression of the phonon modes belonging to the oscillations in the octahedron FeO_6 indicates the substantial content of the ions Fe^{4+} . At the same time, no line of two-magnon scattering indicates absence of antiferromagnetic ordering at room temperature.

4. Conclusions

It has been found out that at room temperature the unannealed initial sample $\text{La}_{0.5}\text{Sr}_{0.5}\text{FeO}_{3-\delta}$ is in the paramagnetic state. The reduction of the temperature to the Néel point $T_N \approx 230 \text{ K}$ results in the appearance of the weak „parasitic“ ferromagnetism. Further reduction of the temperature to the Verwey point $T_V \approx 195 \text{ K}$ results in suppression of the electron transfer process. Experimental evidence supports frustration of the spin state with freezing of the spin glass within the temperature range from 170 to 80 K. The sample $\text{La}_{0.5}\text{Sr}_{0.5}\text{FeO}_{3-\delta}$ annealed in vacuum is in the magnetic-ordered state at room temperature, and with decrease of the temperature the effect of localization of the charge carriers is not detected. Besides, vacuum annealing results in noticeable increase in the Néel temperature.

Acknowledgments

The authors would like to thank M.V. Zhidkova for help in the magnetometric studies.

Funding

The study was supported by the Ministry of Science and Higher Education of the Russian Federation within the framework of State assignments of the Federal Research Center for Problems of Chemical Physics and Medical Chemistry of the RAS (the registered number 124013100858-3) and Osipyan Institute of Solid State Physics of the RAS.

Conflict of interest

The authors declare that they have no conflict of interest.

References

- [1] J. Blasco, B. Aznar, J. Garcia, G. Subias, J. Herrero-Martín, J. Stankiewicz. *Phys. Rev. B* **77**, 5, 054107 (2008).
- [2] R.J. McQueeney, J. Ma, S. Chang, J.-Q. Yan, M. Hehlen, F. Trouw. *Phys. Rev. Lett.* **98**, 12, 126402 (2007).
- [3] F. Gao, P.L. Li, Y.Y. Weng, S. Dong, L.F. Wang, L.Y. Lv, K.F. Wang, J.-M. Liu. *Appl. Phys. Lett.* **91**, 7, 072504 (2007).
- [4] T. Ishikawa, S.K. Park, T. Katsufuji, T. Arima, Y. Tokura. *Phys. Rev. B* **58**, 20, R13326 (1998).
- [5] D.D. Taylor, N.J. Schreiber, B.D. Levitas, X. Wenqian, P.S. Whitfield, E.E. Rodriguez. *Chem. Mater.* **28**, 11, 3951 (2016).
- [6] V.L. Kozhevnikov, I.A. Leonidov, M.V. Patrakeev, A.A. Markov, Y.N. Blinovskov. *J. Solid State Electrochem.* **13**, 3, 391 (2009).
- [7] C. Batiot-Dupeyrat, F. Martinez-Ortega, M. Ganneb, J.M. Taibouët. *Appl. Catal. A* **206**, 2, 205 (2001).
- [8] J.B. Goodenough. *Magnetism and The Chemical Bond*. Interscience Publishers. N.Y. (1963). 393 p.
- [9] M. Eibschütz, S. Shtrikman, D. Treves. *Phys. Rev.* **156**, 2, 562 (1967).
- [10] M. Takano, T. Okita, N. Nakayama, Y. Bando, Y. Takeda, O. Yamamoto, J.B. Goodenough. *J. Solid State Chem.* **73**, 1, 140 (1988).
- [11] T. Mizokawa, A. Fujimori. *Phys. Rev. Lett.* **80**, 6, 1320 (1998).
- [12] M. Takano, J. Kawachi, N. Nakanishi, Y. Takeda. *J. Solid State Chem.* **39**, 1, 75 (1981).
- [13] J. Matsuno, T. Mizokawa, A. Fujimori, Y. Takeda, S. Kawasaki, M. Takano. *Phys. Rev. B* **66**, 19, 193103 (2002).
- [14] J.B. Yang, W.B. Yelon, W.J. James. *Phys. Rev. B* **66**, 18, 184415 (2002).
- [15] V.D. Sedykh, O.G. Rybchenko, N.V. Barkovsky, A.I. Ivanov, V.I. Kulakov. *FTF* **63**, 10, 1648 (2021). (in Russian).
- [16] K.A. Gavrilicheva, O.I. Barkalov, V.D. Sedykh. *Bull. Russ. Acad. Sci. Phys.* **87**, Suppl. 1, S36 (2023).
- [17] V. Sedykh, V. Rusakov, O. Rybchenko, A. Gapochka, K. Gavrilicheva, O. Barkalov, S. Zaitsev, V. Kulakov. *Ceram. Int.* **49**, 15, 25640 (2023).
- [18] M.E. Matsnev, V.S. Rusakov. *AIP Conf. Proc.* **1489**, 1, 178 (2012).
- [19] J.B. Yang, X.D. Zhou, Z. Chu, W.M. Hikal, Q. Cai, J.C. Ho, D.C. Kundaliya, W.B. Yelon, W.J. James, H.U. Anderson, H.H. Hamdeh, S.K. Malik. *J. Phys: Condens. Matter.* **15**, 29, 5093 (2003).
- [20] J. Li, X. Kou, Y. Qin, H. He. *Phys. Status Solidi A* **191**, 1, 255 (2002).
- [21] G. Li, L. Li, M. Zhao. *Phys. Status Solidi B* **197**, 1, 165 (1996).
- [22] F. Millange, S. de Brion, G. Chouteau. *Phys. Rev. B* **62**, 9, 5619 (2000).
- [23] J.T. Phong, D.H. Manh, L.H. Nguyen, D.K. Tung, N.X. Phuc, I.-J. Lee. *J. Magn. Magn. Mater.* **368**, 240 (2014).
- [24] X.N. Ying, L. Zhang. *Solid State Commun.* **152**, 14, 1252 (2012).
- [25] G.B. Wright. *Light Scattering Spectra of Solids*. Springer Berlin, Heidelberg (1969). 763 p.
- [26] O.I. Barkalov, S.V. Zaitsev, V.D. Sedykh. *Solid State Commun.* **354**, 1, 114912 (2022).
- [27] M.O. Ramirez, M. Krishnamurthi, S. Denev, A. Kumar, S.-Y. Yang, Y.-H. Chu, E. Saiz, J. Seidel, A.P. Pyatakov, A. Bush, D. Viehland, J. Orenstein, R. Ramesh, V. Gopalan. *Appl. Phys. Lett.* **92**, 2, 022511 (2008).
- [28] M.C. Weber, M. Guennou, H.J. Zhao, J. Iniguez, R. Vilarinho, A. Almeida, J.A. Moreira, J. Kreisel. *Phys. Rev. B* **94**, 21, 214103 (2016).

Translated by M.Shevelev